DMD Fast Forward. Published on June 6, 2016 as DOI: 10.1124/dmd.116.071084
This article has not been copyedited and formatted. The final version may differ from this version.

USE OF HUMAN PLASMA SAMPLES TO IDENTIFY CIRCULATING DRUG METABOLITES THAT INHIBIT CYTOCHROME P450 ENZYMES

Heather Eng and R. Scott Obach

Pfizer Inc.

Groton, CT, USA

Downloaded from dmd.aspetjournals.org at ASPET Journals on June 18, 2019

DMD Fast Forward. Published on June 6, 2016 as DOI: 10.1124/dmd.116.071084
This article has not been copyedited and formatted. The final version may differ from this version.

Running Title: Ex Vivo Evaluation of P450 Inhibition

Author for Correspondence:

R. Scott Obach

Pfizer Inc.

Groton, CT, USA, 06340

Email: r.scott.obach@pfizer.com

Number of:

Text pages: 16

Tables: 2

Figures: 8

References: 31

Number of words in:

Abstract: 219

Introduction: 601

Discussion: 1195

Abbreviations: P450, cytochrome P450; HPLC-MS, high pressure liquid chromatography-mass spectrometry; PBPK, physiologically-based pharmacokinetic; DDI, drug-drug interaction; NADPH, reduced nicotinamide adenine dinucleotide phosphate.

Downloaded from dmd.aspetjournals.org at ASPET Journals on June 18, 2019

DMD Fast Forward. Published on June 6, 2016 as DOI: 10.1124/dmd.116.071084
This article has not been copyedited and formatted. The final version may differ from this version.

ABSTRACT

Drug interactions elicited through inhibition of cytochrome P450 enzymes are important in pharmacotherapy. Recently, greater attention has been focused on not only parent drugs inhibiting P450 enzymes, but also possible inhibition of these enzymes by circulating metabolites. In this report, an ex vivo method whereby the potential for circulating metabolites to be inhibitors of P450 enzymes is described. To test this method, seven drugs and their known plasma metabolites were added to control human plasma at concentrations previously reported to occur in humans following administration of the parent drug. A volume of plasma for each drug based on the known inhibitory potency and C_{avg} of the parent drug, was extracted and fractionated by HPLC-MS, and the fractions were tested for inhibition of six human P450 enzyme activities (CYP1A2, 2C8, 2C9, 2C19, 2D6, and 3A4). Observation of inhibition in fractions that correspond to the retention times of metabolites indicate that the metabolite has the potential to contribute to P450 inhibition in vivo. Using this approach, norfluoxetine, hydroxyitraconazole, desmethyldiltiazem, desacetyldiltiazem, desethylamiodarone, hydroxybupropion, erythro-dihydrobupropion, and threo-dihydrobupropion were identified as circulating metabolites that inhibit P450 activities at similar or greater extent as the parent drug. A decision tree is presented outlining how this method can be used to determine when a deeper investigation of the P450 inhibition properties of a drug metabolite is warranted.

Downloaded from dmd.aspetjournals.org at ASPET Journals on June 18, 2019

DMD Fast Forward. Published on June 6, 2016 as DOI: 10.1124/dmd.116.071084
This article has not been copyedited and formatted. The final version may differ from this version.

INTRODUCTION

Drug-drug interactions (DDIs) that arise via inhibition of cytochrome P450 enzymes are important in pharmacotherapy. Through extensive research over the past three decades, the science underlying this mechanism of DDIs is well understood (Rodrigues, 2008). The extent of our understanding of CYP-based DDIs is so great that current practices of relating in vitro enzyme inhibition data to in vivo DDI outcomes now leverage sophisticated physiologically based pharmacokinetic (PBPK) modelling approaches that can test DDI hypotheses using different subsets of subject populations (Varma, et al., 2015).

Nevertheless, despite this depth of understanding, specific examples exist that demonstrate that there can be DDIs that are not necessarily expected. One such possibility is when a metabolite of a drug, not the drug itself, is the entity responsible for inhibition of a P450 enzyme. For example, gemfibrozil glucuronide has been shown to be responsible for serious DDIs with cerivastatin via inhibition of CYP2C8, while the parent drug gemfibrozil does not inhibit that enzyme (Shitara, et al., 2004; Oglivie, et al., 2006). Bupropion metabolites are putatively responsible for inhibition of CYP2D6 mediated clearance of desipramine while the parent drug is not (Reese, et al., 2008). In other cases, a metabolite can add to the inhibition of a P450 enzyme already inhibited by the parent drug. Itraconazole inhibits CYP3A and causes DDI, and metabolites of itraconazole can add to this inhibition (Ke, et al., 2014). While examples of drug metabolites being responsible for DDI are rare (Yeung, et al., 2011; Yu and Tweedie, 2013; Callegari, et al., 2013), they nevertheless can be important such that government pharmaceutical regulatory authorities now recommend that metabolites having exposure at 25% of that of parent and/or representing 10% of total drug-related material in human circulation be

Downloaded from dmd.aspetjournals.org at ASPET Journals on June 18, 2019

DMD Fast Forward. Published on June 6, 2016 as DOI: 10.1124/dmd.116.071084
This article has not been copyedited and formatted. The final version may differ from this version.

tested for their potential to inhibit drug metabolizing enzymes (FDA, 2012; EMA, 2013, MHLW, 2014).

In the development of new drugs, it is common practice to test these compounds for their potential to inhibit P450 enzymes before administration to humans for the first time. However it is not common to test drug metabolites for this property at that time due to the fact that the circulating metabolites in human would not yet be known. In vitro drug metabolism experiments using human-derived reagents (liver microsomes, hepatocytes, etc.) can yield dozens of metabolites, but it is challenging to predict those that would be present in circulation at specific concentrations (Loi, et al., 2013; Lutz and Isoherranen, 2012; Nguyen, et al., 2016). When human subjects are dosed with a new drug candidate for the first time, modern bioanalytical approaches, such as high resolution mass spectrometry, can offer considerable qualitative insight into the identities of important circulating metabolites. From that information, possible metabolite structures can be synthesized and verified. With authentic standards of metabolites in hand, each can be tested for their potential to inhibit P450 enzymes, their plasma concentrations can be measured, and the data can be used in the aforementioned PBPK models to predict DDI. However, this is a lengthy and convoluted process, and in the vast majority of cases the likely outcome will be that the metabolite(s) will not have any effect (Yu and Tweedie, 2013; Callegari, et al., 2013). To this end, we have developed a method whereby human plasma samples from subjects dosed with the drug candidate can be used to test for inhibition of cytochrome P450, thereby obviating the need for identification, synthesis, testing and measurement of plasma concentrations of metabolites. This approach (termed “activity-grams”) was previously used to find pharmacologically active metabolites (Sawant-Basak, et al., 2013; Obach, 2013; Walker, et al, 2014). It has now been applied for P450 inhibition using

Downloaded from dmd.aspetjournals.org at ASPET Journals on June 18, 2019

DMD Fast Forward. Published on June 6, 2016 as DOI: 10.1124/dmd.116.071084
This article has not been copyedited and formatted. The final version may differ from this version.

control human plasma to which relevant concentrations of drug and metabolite(s) for seven drugs were added. The method and results are described herein.

Downloaded from dmd.aspetjournals.org at ASPET Journals on June 18, 2019

DMD Fast Forward. Published on June 6, 2016 as DOI: 10.1124/dmd.116.071084
This article has not been copyedited and formatted. The final version may differ from this version.

MATERIALS AND METHODS

Materials. Heterologously expressed recombinant DNA derived human cytochrome P4501A2, 2C9, 2D6, and 3A4 enzymes coexpressed with P450 oxidoreductase were obtained from Panvera Corporation (Madison, WI). P4502C8 and 2C19 coexpressed with both oxidoredctase and cytochrome b5 were from BD Gentest (Woburn, MA). Hydroxyitraconazole, norfluoxetine, *erythro*-hydrobupropion, *threo*-hydrobupropion, desmethylcitalopram, didesmethylcitalopram, desacetyldiltiazem, and desmethyldiltiazem were from Toronto Research Chemicals (Toronto, Ontario, Canada). NADPH, itraconazole, fluoxetine, citalopram, diltiazem, bupropion, gemfibrozil, amiodarone, tacrine, amodiaquine, diclofenac, dextromethorphan, and dextrorphan were from Sigma-Aldrich (St. Louis, MO). (S)-mephenytoin was from Biomol (Plymouth Meeting, PA). Bupropion, 4-hydroxybupropion, and (S)-4'-hydroxymephenytoin were from Syncom (Groningen, Netherlands). 1-Hydroxytacrine, desethylamodiaquine, midazolam, [$^{2}H_{3}$]1-hydroxytacrine, [$^{2}H_{5}$]N-desethylamodiaquine, [$^{2}H_{3}$]dextrorphan, [$^{2}H_{4}$]1'-hydroxymidazolam were prepared under contract by Cerilliant Corp. (Austin, TX). [$^{2}H_{3}$](S)-4'-hydroxymephenytoin, [$^{13}C_{6}$]4'-hydroxydiclofenac, 4'-hydroxydiclofenac, and 1'-hydroxymidazolam were prepared at Pfizer. Gemfibrozil acyl glucuronide was custom synthesized at Wuxi App Tec (Shanghai, China).

Human Plasma Samples. Control human plasma (BioreclamationIVT, Baltimore, MD) was spiked from 5 mM stock solutions of drugs and metabolites in acetonitrile or water to final concentrations representative of time-averaged concentrations (C_{avg}) in humans at normal therapeutic dose levels. These are listed in Table 1.

Downloaded from dmd.aspetjournals.org at ASPET Journals on June 18, 2019

DMD Fast Forward. Published on June 6, 2016 as DOI: 10.1124/dmd.116.071084
This article has not been copyedited and formatted. The final version may differ from this version.

Human Plasma Sample Extraction and Fractionation. Method 1. To a volume of plasma containing the parent drug and metabolites was added four volumes of CH_3CN. The volume of plasma extracted was determined using the following equation:

$$\text{volume of plasma to extract} = \frac{4 \bullet 10 \bullet \text{P450 activity assay volume} \bullet IC_{50}}{C_{avg}} \quad \text{(Eq. 1)}$$

in which the IC_{50} and C_{avg} for parent drug are in units of μM (nmol/mL) and the assay volume is 0.1 mL. The extraction volume was calculated this way to target the presence of enough of the parent drug in the inhibition assay to yield approximately 90% inhibition of the most potently inhibited P450 enzyme (i.e. factor of 10 in the equation), assuming incomplete extraction efficiency and elution of the parent into two HPLC fractions (i.e. factor of 4 in the equation). The mixture was mixed vigorously, spun in a centrifuge (Jouan, St. Herblen, France) at 1700 g for 5 min, and the supernatant was transferred to a vacuum centrifuge (Genevac EZ-2, Valley Cottage, NY). The supernatant was evaporated under the HPLC solvent setting at 40°C or less. To the dried residue was added 1% formic acid in water containing 10% CH_3CN (100 μL). The sample was injected onto an HPLC-MS system (Thermo-Finnigan LTQ ion trap mass spectrometer equipped with a Surveyor quaternary HPLC pump, degasser, autoinjector, and diode array UV-VIS detector, Thermo-Fisher, Waltham, MA). Separation was effected on a Polaris C18 column (4.6 x 250 mm, 5μm particle size, Agilent Technologies, Santa Clara, CA) using a mobile phase of 0.1% formic acid in water and CH_3CN. The flow rate was set at 0.8 mL/min and the mobile phase gradient was programmed to optimize the separation of the parent drug from its respective metabolites in a 40 min run time. The UV-VIS detector monitored absorbance of wavelengths from 200-400 nm. The flow emanating from the UV-VIS detector was split at a ratio of ~15:1, with the smaller portion introduced into the mass spectrometer and the majority going to a fraction collector (CTC-PAL, Leap Technologies, Carrboro, NC). The

Downloaded from dmd.aspetjournals.org at ASPET Journals on June 18, 2019

DMD Fast Forward. Published on June 6, 2016 as DOI: 10.1124/dmd.116.071084
This article has not been copyedited and formatted. The final version may differ from this version.

mass spectrometer was operated in the positive mode. Source potentials and setting were adjusted to optimize the signal for the parent drug. MS^1, MS^2, and MS^3 data were collected, with the latter in data-dependent scanning mode of the two most abundant ions detected. In the case of gemfibrozil, the mass spectrometer was operated in the negative ion mode, and a post-column, post-split infusion of ammonium hydroxide (30% at 1 µL/min) was connected to the eluent entering the mass spectrometer.

Fractions were collected into 96-well polypropylene 1.2 mL cluster tubes at 30 sec intervals. Collection commenced at 6 min post-injection to avoid bulk materials eluting in the void volume until 40 min post-injection. The fractions were transferred to the Genevac vacuum centrifuge and the solvent removed by evaporation. For itraconazole and gemfibrozil, fractions were collected into a 96-well block containing glass inserts that had been subjected to gas phase silylation to reduce the potential for non-specific adsorption.

For each plasma sample processed that contained drug and metabolite(s) mixture, a corresponding control plasma sample was processed in parallel.

Human Plasma Sample Extraction Method 2. For drugs requiring a larger volume of plasma to extract (based on the calculation made in equation 1), an alternate solid-phase extraction (SPE) method was used. Waters Oasis cartridges (HLB, 6g, 35 mL, 60 µm particle size, Waters, Milford, MA) were preconditioned using 40 mL methanol, followed by 40 mL 1% formic acid in water. Formic acid was added to plasma samples (up to 20 mL volume) to a final concentration of 1%, and these were applied to the SPE cartridge. The cartridge was washed with 10% CH_3CN in 1% aqueous formic acid (40 mL) followed by elution with 80% CH_3CN in 1% aqueous formic acid (40 mL). The eluent was evaporated in a vacuum centrifuge as above, and all further processing and fractionation was done as in Method 1.

Downloaded from dmd.aspetjournals.org at ASPET Journals on June 18, 2019

DMD Fast Forward. Published on June 6, 2016 as DOI: 10.1124/dmd.116.071084
This article has not been copyedited and formatted. The final version may differ from this version.

Inhibition Assay. To tubes containing dried fractions was added 0.05 mL of a mixture containing buffer, $MgCl_2$, NADPH, and substrates. These were subjected to sonication for 10 min and then pre-warmed in a 96-well heating block at 37°C for 5 min. To these tubes was added a mixture of six recombinant P450 enzymes in 0.05 mL. Final incubation concentrations were as follows: CYP1A2 (6.6 pmol/mL), CYP2C8 (0.67 pmol/mL), CYP2C9 (3.7 pmol/mL), CYP2C19 (55 pmol/mL), CYP2D6 (1.0 pmol/mL), CYP3A4 (2.2 pmol/mL), tacrine (3.0 µM), amodiaquine (1.0 µM), diclofenac (3.0 µM), S-mephenytoin (20 µM), dextromethorphan (0.5 µM), midazolam (1.0 µM), potassium phosphate (0.1 M, pH 7.45), $MgCl_2$ (3.3 mM), and NADPH (1.3 mM). Incubations were carried out for 8 min and terminated by addition of 0.3 mL of an internal standard mixture in formic acid/CH_3CN (0.1:99.9). Internal standards in the termination solution were at the following concentrations: [$^2H_3$]1-hydroxytacrine (5 nM), [$^2H_5$]N-desethylamodiaquine (5 nM), [$^{13}C_6$]4'-hydroxydiclofenac (20 nM), [$^2H_3$](S)-4'-hydroxymephenytoin (50 nM), [$^2H_3$]dextrorphan (5 nM), and [$^2H_4$]1'-hydroxymidazolam (20 nM). Samples were centrifuged at 2300 xg for 5 minutes. 300 µL of supernatant was dried using a nitrogen gas evaporator, followed by reconstitution in 150 µl formic acid/CH_3CN/water (0.1/10/89.9). The HPLC-MS system consisted of an AB Sciex (Framingham, MA) triple quadrupole mass spectrometer with a TurboIonSpray source and a Waters Acquity autosampler and UPLC system. Analytes were separated using a Halo C18 2.0 µm 2.1x5 mm column. Mobile phase A was 0.1% formic acid in water and mobile phase B 0.1% formic acid in acetonitrile. The following program describes %B in the mobile phase: hold at 10% 0-0.1 min, ramp to 70% from 0.1-2.0 min, ramp to 95% from 2.0-2.1 min and hold at 95% through 2.35 min, step to 10% at 2.4 min and hold for column equilibration. Sample injection volume was 10 µl and the flow rate was 0.5 mL/min. The MS was operated in multiple reaction mode (MRM)

Downloaded from dmd.aspetjournals.org at ASPET Journals on June 18, 2019

DMD Fast Forward. Published on June 6, 2016 as DOI: 10.1124/dmd.116.071084
This article has not been copyedited and formatted. The final version may differ from this version.

with scheduled MRM (40 sec detection window). Samples were monitored for metabolites and internal standards; m/z transitions and retention times were: desethylamodiaquine (328.2→282.9, 0.56 min), [$^2H_5$]N-desethylamodiaquine (333.2→283.0, 0.56 min), 1-hydroxytacrine (215.1→197.1, 0.55 min), [$^2H_3$]1-hydroxytacrine (218.1→200.2, 0.55 min), dextrorphan (258.1→201.1, 0.81 min), [$^2H_3$]dextrorphan (261.1→201.1, 0.81 min), (S)-4'-hydroxymephenytoin (235.2→150.1, 0.95 min), [$^2H_3$](S)-4'-hydroxymephenytoin (239.1→151.0, 0.95 min), 1'-hydroxymidazolam (342.1→323.9, 1.09 min), [$^2H_4$]1'-hydroxymidazolam (346.1→328.0, 1.09 min), 4'-hydroxydiclofenac (311.8→266.1, 1.67 min), and [$^{13}C_6$]4'-hydroxydiclofenac (318.0→272.0, 1.67 min).

Data was analyzed using Analyst 1.6 or MultiQuant 3.0 (AB Sciex). Standards of each probe metabolite were fit by least squares regression with $1/x^2$ weighting and unknown concentrations were determined from the resulting best-fit equation. Standard concentrations were selected to ensure metabolite formation was within the linear dynamic range of the instrument. Percent inhibition versus control wells was calculated in Microsoft Excel (Redmond, WA).

The evaporated fractions from HPLC occupied 68 tubes. Four tubes were used as the controls (no fraction) and 16 tubes were used to construct the standard curves. Four tubes were used as positive controls wherein the parent drug for each run was added in 0.1% formic acid in 50% CH_3CN at a concentration such that there would be expected to be 75% inhibition of the most potently inhibited enzyme. These tubes were subjected to evaporation with the HPLC fractions. This serves as a check that the reconstitution process adequately redissolved the drug.

Downloaded from dmd.aspetjournals.org at ASPET Journals on June 18, 2019

DMD Fast Forward. Published on June 6, 2016 as DOI: 10.1124/dmd.116.071084
This article has not been copyedited and formatted. The final version may differ from this version.

RESULTS

The seven parent drugs used to develop this approach were first tested for their abilities to inhibit the six CYP enzyme activities. IC_{50} values are listed in Table 2, and are consistent with values previously described in the scientific literature.

CYP inhibition activity-grams are shown in Figures 1-7. Among the drugs tested, four general outcomes were observed: (1) a metabolite(s) contributes a greater inhibition than the parent drug for one or more enzymes (bupropion metabolites, desacetyldiltiazem); (2) metabolites have relevant/similar contributions as the parent drug (fluoxetine, itraconazole, diltiazem, amiodarone), (3) parent and metabolites essentially lack DDI (citalopram), and (4) inconclusive result due to technical problems (gemfibrozil).

Bupropion is metabolized by hydroxylation as well as reduction of the ketone moiety to isomeric alcohol metabolites. The metabolites circulate at greater concentrations than the parent drug (Table 1), with hydroxybupropion at over 30-fold the parent. Based on the concentration and inhibitory potency of bupropion, a maximum 20 mL plasma sample containing parent drug and metabolites at clinically relevant concentrations was processed by Method 2 and fractionated by HPLC. Hydroxybupropion eluted in a large broad peak at 19.3 min, with bupropion and the two reduced metabolites eluting afterward at 23.0, 23.9, and 24.8 min (Figure 1). Activity-grams for CYP2C19, 2D6, and 3A4 inhibition are shown in Figure 1. (No effects were observed for the other enzymes.) In the activity-grams, the inhibition caused by HPLC fractions of the plasma extracts are plotted for both the control and dosed plasma; thus the control can be used to establish the background noise of the assay as well as any endogenous plasma materials that could be inhibitory (see other examples below). Marked inhibition was observed corresponding to the metabolite peaks for CYP2C19 and 2D6. Bupropion coadministration with CYP2D6

Downloaded from dmd.aspetjournals.org at ASPET Journals on June 18, 2019

DMD Fast Forward. Published on June 6, 2016 as DOI: 10.1124/dmd.116.071084
This article has not been copyedited and formatted. The final version may differ from this version.

cleared drugs has been shown to have an important effect and this has been proposed to occur via the metabolites (Reese, et al., 2008; Kotlyar, et al., 2005). The activity-gram approach with human plasma corroborates this. Also, the data suggest that bupropion administration could cause DDI for drugs cleared by CYP2C19 via its metabolites. A small peak of inhibition was also observed in the CYP3A4 activity-gram corresponding to hydroxybupropion. While the intrinsic inhibitory potency of bupropion metabolites may not be greater than bupropion itself, the inhibition would be expected to be elicited via their higher concentrations in vivo.

Diltiazem and desmethyldiltiazem are known to be CYP3A mechanism-based inactivators and diltiazem coadministration with CYP3A cleared drugs results in DDI. A human plasma sample (20 mL) containing diltiazem, desmethyldiltiazem, and desacetyldiltiazem at clinically relevant plasma concentrations (Table 1) was subjected to processing described in Method 2. HPLC-MS chromatograms and activity-grams for CYP2D6 and CYP3A4 inhibition are shown in Figure 2. Diltiazem and its desmethyl metabolite could not be baseline resolved by HPLC and inhibition of CYP3A4 shown in the activity-gram at 24-25 min could be ascribed to one or both. Also, while the CYP activity assay was designed as a test for reversible inhibition, it was capable of detecting the CYP3A4 inhibition via a mechanism-based inactivator. Desacetyldiltiazem, eluting at 19.1 min, was shown to inhibit CYP2D6 whereas neither diltiazem nor desmethyldiltiazem showed an effect on this enzyme. This offers an example of a metabolite possessing CYP inhibition activity while the parent drug does not. Desacetyldiltiazem has been previously reported to inhibit CYP2D6 and a small DDI has been reported for diltiazem and metoprolol a CYP2D6 substrate (Tateishi, et al., 1989, Molden, et al., 2002). No inhibition peaks were observed in activity-grams for the other enzymes (data not shown).

Downloaded from dmd.aspetjournals.org at ASPET Journals on June 18, 2019

DMD Fast Forward. Published on June 6, 2016 as DOI: 10.1124/dmd.116.071084
This article has not been copyedited and formatted. The final version may differ from this version.

Fluoxetine is known to inhibit CYP2D6 and CYP2C19 (Sager, et al., 2014). The major metabolite of fluoxetine is norfluoxetine, which circulates at a concentration slightly greater than fluoxetine and has a longer half-life. A 2.5 mL sample of plasma containing 1.1 and 1.3 μM of fluoxetine and norfluoxetine, respectively, was subjected to extraction using Method 1. The activity-grams for effects on all six enzymes are shown in Figure 3, along with the ion chromatogram showing the elution of norfluoxetine and fluoxetine at 20.1 and 21.2 min, respectively. CYP2D6 and CYP2C19 showed inhibition peaks coincident with the retention times of both parent and metabolite. In each case, the magnitudes of the two peaks are similar suggesting that the metabolite would likely contribute to drug interactions as much as the parent drug for substrates of these two enzymes. Inhibition was detectable for CYP3A4 and CYP2C8, albeit much lower than for 2D6 and 2C19. Inhibition was not observed for CYP1A2 or 2C9.

Activity-grams for plasma extracts (0.44 mL processed using Method 1) containing itraconazole and hydroxyitraconazole are shown in Figure 4. No inhibition was observed for CYP1A2, 2C9, or 2D6 (not shown) but peaks of inhibition were observed for CYP2C8, 2C19, and 3A4. Preliminary studies showed low inhibition due to poor reconstitution of the dried fractions, consistent with the physicochemical properties of itracaonazole. This necessitated the use of silylated glass tubes for fraction collection, evaporation, reconstitution, and enzyme assay. As expected, peaks of inhibition were observed for both hydroxyitraconazole and itraconazole for CYP3A4 at 18.1 and 27.1 min retention times. Previously reported PBPK modelling of the itraconazole-CYP3A DDI has shown that the metabolite contributes to the effect (Vossen, et al., 2007; Ke, et al., 2014) and this is reinforced by the activity-gram data which shows inhibition peaks for both hydroxyitraconazole and itraconazole. The mobile phase composition used to elute itraconazole had a greater acetonitrile percentage than for other examples. This resulted in

Downloaded from dmd.aspetjournals.org at ASPET Journals on June 18, 2019

DMD Fast Forward. Published on June 6, 2016 as DOI: 10.1124/dmd.116.071084
This article has not been copyedited and formatted. The final version may differ from this version.

the observation of endogenous materials eluting at 29-34 min that inhibited the P450 activities and emphasizes the importance of comparing control and dosed plasma side-by-side.

Amiodarone is a highly lipophilic drug that undergoes N-deethylation. Human plasma (18 mL) spiked with amiodarone and desethylamiodarone at 3.5 and 2.1 μM respectively was extracted using Method 2 and the extract fractionated by HPLC (Figure 5). As with itraconazole, a high percentage of organic modifier was necessary to elute the drug and metabolite, however because there was a greater volume extracted than for itraconazole (see above), there was an even greater degree of interference in the activity-gram at later retention times for all six enzymes. Inhibition peaks were observable in the CYP3A4 activity-gram, however in other enzymes these could not be reliably discerned, albeit there may be some small peaks for desethylamiodarone for some of the other enzymes. The example of amiodarone represents a limitation of this approach regarding the liophilicity of the drug that can be examined.

Citalopram is known to not cause DDI via inhibition of P450 enzymes, and with its two circulating N-demethylated metabolites it was used as a negative control for the approach. The maximum volume of plasma (20 mL) containing citalopram, desmethylcitalopram, and didesmethylcitalopram at clinically relevant concentrations was extracted using Method 2 and fractionated by HPLC. Retention times for citalopram and its two metabolites were 28.6, 27.8, and 26.9 min, respectively. No effect on any of the six P450 enzyme activities tested was observed in fractions eluting in this retention time region (Figure 6).

Gemfibrozil and its glucuronide metabolite posed the greatest challenge to the method. The resulting CYP inhibition activity grams contained several interfering peaks of inhibition (Figure 7) and made most of the data uninterpretable. A small peak of inhibition can be discerned in the CYP2C8 activity-gram corresponding to the elution of gemfibrozil glucuronide,

Downloaded from dmd.aspetjournals.org at ASPET Journals on June 18, 2019

DMD Fast Forward. Published on June 6, 2016 as DOI: 10.1124/dmd.116.071084
This article has not been copyedited and formatted. The final version may differ from this version.

however this signal is not reliable enough to identify the metabolite as an inhibitor. Additionally, the activity-gram had endogenous interferences in the extract eluting near gemfibrozil, preventing detection of a signal of inhibition and rendering the result as inconclusive (see Figure 8 and below). This example illustrates the value of the parent compound serving as its own positive control through in that the absence of observation of inhibition of CYP2C19 by gemfibrozil successfully identified that the approach was not useable in this case. Investigation of the failure could not conclusively demonstrate a reason, however it was shown that gemfibrozil and the glucuronide were successfully extracted, fractionated, and reconstituted, but that concentrations after incubation were lower than expected.

Downloaded from dmd.aspetjournals.org at ASPET Journals on June 18, 2019

DMD Fast Forward. Published on June 6, 2016 as DOI: 10.1124/dmd.116.071084
This article has not been copyedited and formatted. The final version may differ from this version.

DISCUSSION

The method described in this report offers a viable shortcut approach to evaluating whether circulating drug metabolites could have a meaningful contribution to DDI, without the need of obtaining authentic standards of metabolites and testing each of them individually. A suggested logic tree for insertion of this method into the drug development process is shown in Figure 8. It is dependent on three pieces of information that would ordinarily be known at the time that human plasma samples from subjects dosed with a new drug candidate are available such that the method could be employed: (a) in vitro potency of the parent drug against CYP enzyme activities, (b) the concentration of the parent drug in plasma, and (c) HPLC-MS conditions that would have been developed and used to qualitatively characterize the metabolite profile in human plasma samples. With that knowledge in hand, a volume of plasma from dosed human subjects can be selected for extraction and fractionation, and the fractions tested for CYP inhibition using the method described in this report.

If peaks of inhibition are observed that are not eluting where the parent drug elutes, it suggests that there is a plasma metabolite that inhibits a CYP activity. Since the abundance of the metabolite is not known, the inhibition could be due to a minor metabolite that is very potent or a very abundant metabolite that is less potent. Irrespective of low abundance/high potency or high abundance/low potency, the data would suggest that there could be inhibition in vivo. Positive findings from the ex vivo activity-gram would lead to a deeper investigation of the metabolite, delineating it as one worthy of the investment to synthesize and test it. However, if there are no other peaks of inhibition in the activity-gram except for the parent drug, then the approach has shown that no further work on metabolites as inhibitors of P450 enzymes is needed. Based on an analysis of known drugs (Yeung, et al., 2011; Yu and Tweedie, 2013;

Downloaded from dmd.aspetjournals.org at ASPET Journals on June 18, 2019

DMD Fast Forward. Published on June 6, 2016 as DOI: 10.1124/dmd.116.071084
This article has not been copyedited and formatted. The final version may differ from this version.

Callegari, et al., 2013), it can be anticipated that this latter result will be the more frequent outcome and thus this method can be employed as a quick and resource-sparing approach to reliably obtain this outcome.

A volume of 20 mL is the maximum that can feasibly be evaluated using this approach. For parent drugs that do not inhibit CYP enzymes (or are weak), this maximum volume can be used and if there are no inhibition peaks, then it is likely that DDI will not be of concern (as illustrated by the citalopram data). For lipophilic drugs, the HPLC mobile phase composition needed for elution is such that endogenous plasma materials will also elute that can show CYP inhibition. This was observed in the examples of itraconazole, gemfibrozil, and amiodarone, and in the latter case was very pronounced because a high volume of plasma needed to be processed. (As an aside, initial attempts were made to merely test whole plasma extracts containing parent drug vs those containing parent drug plus metabolite for CYP inhibition as a means to identify the potential for metabolites to contribute to inhibition. These attempts failed because even plasma that did not contain drug or metabolites showed considerable inhibition. This necessitated the use of HPLC to resolve drug and metabolites from these endogenous materials. The identities of these plasma endogenous materials are unknown.) Thus, this method is likely not applicable in an example like amiodarone because of this observation, as well as the greater challenge of ensuring that lipophilic drugs and metabolites are suitably re-dissolved from the dried fractions when reconstituting in CYP assay buffer. In an example such as amiodarone, the more conventional approach of synthesizing and testing individual metabolites would be warranted, or alternate sample work-up procedure and chromatographic methods may be needed In the case of itraconazole, the hydroxy metabolite was readily identifiable as a contributor to CYP3A4 inhibition, and would have triggered a closer examination of this metabolite. And like

Downloaded from dmd.aspetjournals.org at ASPET Journals on June 18, 2019

DMD Fast Forward. Published on June 6, 2016 as DOI: 10.1124/dmd.116.071084
This article has not been copyedited and formatted. The final version may differ from this version.

the example of itraconazole/hydroxyitraconazole, the example of fluoxetine/norfluoxetine also illustrates that a metabolite can contribute, with the parent drug, to a DDI. This would be particularly salient if, using PBPK modelling, the parent drug alone is not projected to cause a DDI, but the combination of parent and metabolite would be enough to predict a DDI.

In the examples of bupropion and diltiazem, the method showed that metabolites of these drugs can be responsible for DDI. Hydroxybupropion is present in much higher concentration in plasma than bupropion and thus inhibition of CYP2D6 is due to this metabolite. The findings also show that CYP2C19 may be of concern for bupropion and its metabolites. Diltiazem and desmethyldiltiazem were shown to be CYP3A4 inhibitors using the approach, as expected (albeit baseline chromatographic resolution was not attainable for these two compounds). Importantly, desacetyldiltiazem was identified as a CYP2D6 inhibitor using this approach, which had been reported previously (Molden, et al., 2002). If this approach were used prospectively, it would have directed a closer examination of desacetyldiltiazem as a possible CYP2D6 inhibitor.

The examples of amiodarone and gemfibrozil show the limits of the method whereas the other examples offer a clear picture of the inhibition potential of metabolites. It will thus be important when using this approach in a truly prospective manner to carefully evaluate the robustness of the data with regard to interferences from endogenous plasma components. Gemfibrozil glucuronide, a mechanism-based inactivator of CYP2C8, was not identified using the method, however there was also no inhibition of CYP2C19 where gemfibrozil itself eluted indicating an inconclusive study (Figure 8). In such a case, investigation of the potential for circulating metabolites to inhibit P450 enzymes would need to be done directly using a synthesized standard(s) of the metabolite(s).

Downloaded from dmd.aspetjournals.org at ASPET Journals on June 18, 2019

DMD Fast Forward. Published on June 6, 2016 as DOI: 10.1124/dmd.116.071084
This article has not been copyedited and formatted. The final version may differ from this version.

In summary, a method is described whereby the potential for circulating drug metabolites to inhibit important P450 enzymes can be assessed. Knowledge of the identities and plasma concentrations of individual metabolites is not required, nor does an authentic standard need to be made. (In some cases, chemical synthesis of drug metabolites can be extremely challenging.) Since actual plasma samples from humans dosed with the parent drug are used as the source material, the findings should be meaningful for understanding whether a DDI concern is truly warranted, since metabolites would be present at pertinent concentrations relative to the parent drug. Observation of an inhibition peak in an activity-gram where a metabolite elutes would lead to a more standard investigation of the metabolite as an inhibitor (i.e. synthesis, measurement of plasma protein binding, determination of inhibition potency and mechanism, and use of PBPK modelling to project in vivo DDI). Observation of no new inhibition peaks (besides parent drug) would obviate any further investigation. It is important to note that the method is limited to metabolites in circulation and it is possible that a metabolite could be formed in liver and cause P450 inhibition without that metabolite entering the circulation. Nevertheless, this method should be applicable to meet recently added regulatory requirements that not only parent drugs require evaluation for their potential to inhibit drug metabolizing enzymes, but that circulating metabolites be evaluated as well. The potential for application of this approach to other DDI endpoints merits further investigation.

Downloaded from dmd.aspetjournals.org at ASPET Journals on June 18, 2019

DMD Fast Forward. Published on June 6, 2016 as DOI: 10.1124/dmd.116.071084
This article has not been copyedited and formatted. The final version may differ from this version.

Acknowledgements: The authors extend their gratitude to Drs. Larry Tremaine and Li Di for support of this endeavor

Authorship Contributions:

Participated in research design: Eng, Obach

Conducted experiments: Eng, Obach

Performed data analysis: Eng, Obach

Wrote or contributed to the writing of the manuscript: Eng, Obach

Downloaded from dmd.aspetjournals.org at ASPET Journals on June 18, 2019

DMD Fast Forward. Published on June 6, 2016 as DOI: 10.1124/dmd.116.071084
This article has not been copyedited and formatted. The final version may differ from this version.

References

Barone JA, Koh JG, Bierman RH, Colaizzi JL, Swanson KA, Gaffar MC, Moskovitz BL, Mechlinski W, and VandeVelde V (1993) Food interaction and steady-state pharmacokinetics of itraconazole capsules in healthy male volunteers. Antimic. Agents Chemother. 37: 778-784.

Callegari E, Kalgutkar AS, Leung L, Obach RS, Plowchalk DR, Tse S (2013) Drug metabolites as cytochrome P450 inhibitors: a retrospective analysis and proposed algorithm for evaluation of the pharmacokinetic interaction potential of metabolites in drug discovery and development. Drug Metab. Dispos. 41: 2047-2055.

European Medicines Agency (2013) Guideline on the Investigation of Drug Interactions http://www.ema.europa.eu/docs/en_GB/document_library/Scientific_guideline/2012/07/WC500129606.pdf (Accessed 13-February-2016).

Golden RN, DeVane CL, Laizure SC, Rudorfer MV, Sherer MA, and Potter WZ (1988) Bupropion in depression II. the role of metabolites in clinical outcome. Arch. Gen. Psych. 45:145-149.

Hoglund P and Nilsson LG (1989) Pharmacokinetics of diltiazem and its metabolites after single and multiple dosing in healthy volunteers. Ther. Drug Monit. 11: 558-566.

Downloaded from dmd.aspetjournals.org at ASPET Journals on June 18, 2019

DMD Fast Forward. Published on June 6, 2016 as DOI: 10.1124/dmd.116.071084
This article has not been copyedited and formatted. The final version may differ from this version.

Harvey AT and Preskorn SH (2001) Fluoxetine pharmacokinetics and effect on CYP2C19 in young and elderly volunteers. J. Clin. Psychopharmacol. 21: 161-166.

Ke AB, Zamek-Gliszczynski MJ, Higgins JW and Hall SD (2014) Itraconazole and Clarithromycin as Ketoconazole Alternatives for Clinical CYP3A Inhibition Studies. Clin. Pharmacol. Ther. 95: 473–476.

Kotlyar M, Brauer LH, Tracy TS, Hatsukami DK, Harris J, Bronars CA, Adson DE. (2005) Inhibition of CYP2D6 activity by bupropion. J. Clin. Psychopharmacol. 25: 226-229.

Loi CM Smith DA, and Dalvie D (2013) Which metabolites circulate? Drug Metab. Dispos 41: 933-951.

Lutz JD and Isoherranen N. (2012). Prediction of relative in vivo metabolite exposure from in vitro data using two model drugs: dextromethorphan and omeprazole. Drug Metab. Dispos. 40: 159-168.

Ministry of Health, Labour, and Welfare of Japan. (2014) Drug interaction guideline for drug development and labeling recommendations (draft for public comment) http://www.solvobiotech.com/documents/Japanese_DDI_guideline_(draft)_2014Jan.pdf accessed 13-Feb-2016.

Downloaded from dmd.aspetjournals.org at ASPET Journals on June 18, 2019

DMD Fast Forward. Published on June 6, 2016 as DOI: 10.1124/dmd.116.071084
This article has not been copyedited and formatted. The final version may differ from this version.

Molden E, Asberg A, and Christensen H (2002) Desacetyl-diltiazem displays severalfold higher affinity to CYP2D6 compared with CYP3A4. Drug Metab. Dispos. 30: 1-3.

Nguyen HQ, Callegari E, and Obach RS (2016) Mechanistic modeling to predict midazolam metabolite exposure from in vitro data. Drug Metab. Dispos. In press.

Obach RS (2013) Pharmacologically active drug metabolites: impact on drug discovery and pharmacotherapy. Pharmacol. Rev. 65: 578-640.

Ogilvie BW, Zhang D, Li W, Rodrigues AD, Gipson AE, Holsapple J, Toren P, Parkinson A. (2006) Glucuronidation converts gemfibrozil to a potent, metabolism-dependent inhibitor of CYP2C8: Implications for drug-drug interactions. Drug Metab. Dispos. 34: 191-197.

Reese MJ, Wurm RM, Muir KT, Generaux GT, St John-Williams L, McConn DJ (2008)
An in vitro mechanistic study to elucidate the desipramine/bupropion clinical drug-drug interaction. Drug Metab Dispos. 36:1198-201.

Rodrigues AD (Ed.) *Drug-Drug Interactions* (2nd Edition). Informa Healthcare, New York, NY

Sager JE, Lutz JD, Foti RS, Davis C, Kunze KL, and Isoherranen N. (2014) Fluoxetine- and Norfluoxetine-Mediated Complex Drug-Drug Interactions: In Vitro to In Vivo Correlation of Effects on CYP2D6, CYP2C19, and CYP3A4. Clin. Pharmacol. Ther. 95: 653-662.

Downloaded from dmd.aspetjournals.org at ASPET Journals on June 18, 2019

DMD Fast Forward. Published on June 6, 2016 as DOI: 10.1124/dmd.116.071084
This article has not been copyedited and formatted. The final version may differ from this version.

Sawant-Basak A, Coffman KJ, Walker GS, Ryder TF, Tseng E, Miller E, Lee C, Vanase-Frawley MA, Wong JW, Brodney MA, Rapp T, and Obach RS (2013) Metabolism of a serotonin-4 receptor partial agonist 4-{4-[4-tetrahydrofuran-3-yloxy)-benzo[d]isoxazol-3-yloxymethyl]-piperidin-1-ylmethyl}-tetrahydropyran-4-ol (TBPT): identification of an unusual pharmacologically active cyclized oxazolidine metabolite in human. J. Pharm. Sci. 102: 3277-3293.

Shitara Y, Hirano M, Sato H, and Sugiyama Y. (2004) Gemfibrozil and its glucuronide inhibit the organic anion transporting polypeptide 2 (OATP2/OATP1B1:SLC21A6)-mediated hepatic uptake and CYP2C8-mediated metabolism of cerivastatin: analysis of the mechanism of the clinically relevant drug-drug interaction between cerivastatin and gemfibrozil. J Pharmacol Exp Ther. 311: 228-236.

Sindrup SH, Brosen K, Hansen MGJ, Aaes-Jorgensen T, Overoe KF and Gram LF (1993) Pharmacokinetics of citalopram in relation to the sparteine and the mephenytoin oxidation polymorphisms. Ther. Drug Monit. 15: 11-17.

Staubli M, Troendle A, Schmid B, Balmer P, Kohler B, Studer H, and Bircher J (1985) Pharmacokinetics of amiodarone, desethylamiodarone, and other iodine-containing amiodarone metabolites. Eur. J. Clin. Pharmacol. 29: 417-423.

Downloaded from dmd.aspetjournals.org at ASPET Journals on June 18, 2019

DMD Fast Forward. Published on June 6, 2016 as DOI: 10.1124/dmd.116.071084
This article has not been copyedited and formatted. The final version may differ from this version.

Tateishi T, Nakashima H, Shitou T, Kumagai Y, Ohashi K, Hosoda S, and Ebihara A. (1989) Effect of diltiazem on the pharmacokinetics of propranolol, metoprolol and atenolol. Eur. J. Clin. Pharmacol. 36: 67-70.

Tornio A, Niemi M, Neuvonen M, Laitila J, Kalliokoski A, Neuvonen PJ, and Backman JT (2008) The effect of gemfibrozil on repaglinide pharmacokinetics persists for at least 12h after the dose: evidence for mechanism-based inhibition of CYP2C8 in vivo. Clin. Pharmacol. Ther. 84: 403-411.

U.S. Food and Drug Administration (2012) Guidance for Industry. Drug Interaction Studies – Study design, Data Analysis, Implications for Dosing, and Labeling Recommendations. http://www.fda.gov/downloads/drugs/guidancecomplianceregulatoryinformation/guidances/ucm292362.pdf (Accessed 13, February, 2016).

Varma MV, Pang KS, Isoherranen N, and Zhao P (2015) Dealing with the complex drug-drug interactions: Towards mechanistic models. Biopharm. Drug Dispos. 36: 71-92

Vossen M, Sevestre M, Niederalt C, Jang IJ, Willmann S, and Edginton AN (2007) Dynamically simulating the interaction of midazolam and the CYP3A4 inhibitor itraconazole using individual coupled whole-body physiologically-based pharmacokinetic (WB-PBPK) models. Theor. Biol. Med. Model. 4: 13.

Downloaded from dmd.aspetjournals.org at ASPET Journals on June 18, 2019

DMD Fast Forward. Published on June 6, 2016 as DOI: 10.1124/dmd.116.071084
This article has not been copyedited and formatted. The final version may differ from this version.

Wagner C, Pan Y, Hsu V, Grillo JA, Zhang L, Reynolds KS, Sinha V, and Zhao P (2015) Predicting the Effect of Cytochrome P450 Inhibitors on Substrate Drugs: Analysis of Physiologically Based Pharmacokinetic Modeling Submissions to the US Food and Drug Administration. Clin. Pharmacokinet. 54: 117-127

Walker GS, Bauman JN, Ryder TF, Smith EB, Spracklin DK, and Obach RS (2014) Biosynthesis of drug metabolites and quantitation using NMR spectroscopy for use in pharmacologic and drug metabolism studies. Drug Metab. Dispos. 42: 1627-1639. GS

Yeung, C. K.; Fujioka, Y.; Hachad, H.; Levy, R. H.; Isoherranen, N. (2011) Are Circulating Metabolites Important in Drug-Drug Interactions?: Quantitative Analysis of Risk Prediction and Inhibitory Potency. Clin. Pharmacol. Ther.89: 105-113.

Yu H and Tweedie D (2013) A perspective on the contribution of metabolites to drug-drug interaction potential: the need to consider both circulating levels and inhibition potency. Drug Metab. Dispos. 41: 536-540

Downloaded from dmd.aspetjournals.org at ASPET Journals on June 18, 2019

DMD Fast Forward. Published on June 6, 2016 as DOI: 10.1124/dmd.116.071084
This article has not been copyedited and formatted. The final version may differ from this version.

FIGURE LEGENDS

Figure 1. HPLC-MS Traces and CYP Inhibition Activity-Grams for Bupropion and Metabolites in Human Plasma. Top panel: HPLC-MS chromatogram for extracted control human plasma. Second panel: HPLC-MS chromatogram for extracted human plasma containing bupropion and metabolites. Remaining panels: Activity-grams for CYP inhibition by HPLC fractions of the control (red) and dosed (blue) plasma extracts for CYP2C19, CYP2D6 and CYP3A4.

Figure 2. HPLC-MS Traces and CYP Inhibition Activity-Grams for Diltiazem and Metabolites in Human Plasma. Top panel: HPLC-MS chromatogram for extracted control human plasma. Second panel: HPLC-MS chromatogram for extracted human plasma containing diltiazem and metabolites. Remaining panels: Activity-grams for CYP inhibition by HPLC fractions of the control (red) and dosed (blue) plasma extracts for CYP2D6 and CYP3A4.

Figure 3. HPLC-MS Traces and CYP Inhibition Activity-Grams for Fluoxetine and Norfluoxetine in Human Plasma. Top panel: HPLC-MS chromatogram for extracted control human plasma. Second panel: HPLC-MS chromatogram for extracted human plasma containing fluoxetine and norfluoxetine. Remaining panels: Activity-grams for CYP inhibition by HPLC fractions of the control (red) and dosed (blue) plasma extracts.

Figure 4. HPLC-MS Traces and CYP Inhibition Activity-Grams for Itraconazole and Hydroxyitraconazole in Human Plasma. Top panel: HPLC-MS chromatogram for extracted control human plasma. Second panel: HPLC-MS chromatogram for extracted human plasma containing itraconazole and hydroxyitraconazole. Remaining panels: Activity-grams for inhibition of CYP2C8, 2C19, and 3A4 by HPLC fractions of the control (red) and dosed (blue) plasma extracts. Note that the hydroxyitraconazole sample obtained from the vendor had an isomeric impurity eluting at 18.6 min.

Downloaded from dmd.aspetjournals.org at ASPET Journals on June 18, 2019

DMD Fast Forward. Published on June 6, 2016 as DOI: 10.1124/dmd.116.071084
This article has not been copyedited and formatted. The final version may differ from this version.

Figure 5. HPLC-MS Traces and CYP Inhibition Activity-Grams for Amiodarone and Desethylamiodarone in Human Plasma. Top panel: HPLC-MS chromatogram for extracted control human plasma. Second panel: HPLC-MS chromatogram for extracted human plasma containing amiodarone and desethylamiodarone. Remaining panels: Activity-grams for CYP inhibition by HPLC fractions of the control (red) and dosed (blue) plasma extracts.

Figure 6. HPLC-MS Traces and CYP Inhibition Activity-Grams for Citalopram and Metabolites in Human Plasma. Top panel: HPLC-MS chromatogram for extracted control human plasma. Second panel: HPLC-MS chromatogram for extracted human plasma containing citalopram and metabolites. Remaining panels: Activity-grams for CYP inhibition by HPLC fractions of the control (red) and dosed (blue) plasma extracts.

Figure 7. HPLC-MS Traces and CYP Inhibition Activity-Grams for Gemfibrozil and its Acyl Glucuronide Metabolite in Human Plasma. Top panel: HPLC-MS chromatogram for extracted control human plasma. Second panel: HPLC-MS chromatogram for extracted human plasma containing gemfibrozil and gemfibrozil glucuronide. Remaining panels: Activity-grams for CYP2C8 and 2C19 inhibition by HPLC fractions of the control (red) and dosed (blue) plasma extracts. Note that the MS response signal for gemfibrozil was far lower than for the glucuronide in the conditions used.

Figure 8. Decision Tree Scheme for Application of an Ex-Vivo Method for Evaluating the Potential for Circulating Metabolites as CYP Inhibitors.

Downloaded from dmd.aspetjournals.org at ASPET Journals on June 18, 2019

DMD Fast Forward. Published on June 6, 2016 as DOI: 10.1124/dmd.116.071084
This article has not been copyedited and formatted. The final version may differ from this version.

TABLE 1. Human plasma C_{avg} values of drugs and metabolites used in this study.

Drug (Dose)	Drug/Metabolite	C_{avg} (μM)[a]	Reference
Bupropion (200 mg BID)	Bupropion	0.16	Golden et al., 1988
	4-Hydroxybupropion	5.7	
	erythro-Dihydrobupropion	0.44	
	threo-Dihydrobupropion	2.3	
Diltiazem (60 mg TID)	Diltiazem	0.33	Hoglund and Nilsson, 1989
	Desmethyldiltiazem	0.17	
	Desacetyldiltiazem	0.078	
Fluoxetine (40 mg QD)	Fluoxetine	0.76	Harvey and Preskorn, 2001
	Norfluoxetine	0.86	
Itraconazole (200 mg BID)	Itraconazole	2.7	Barone, et al., 1993
	Hydroxyitraconazole	4.7	
Amiodarone (6.3 mg/kg/day)	Amiodarone	3.5	Staubli, et al., 1985
	N-Desethylamiodarone	2.1	
Citalopram (40 mg QD)	Citalopram	0.19	Sindrup, et al., 1993
	Desmethylcitalopram	0.074	
	Didesmethylcitalopram	0.015	
Gemfibrozil (600 mg BID)	Gemfibrozil	35	Tornio, et al., 2008
	Gemfibrozil Glucuronide	23	

[a]C_{avg} was calculated as the AUC(0-τ)/τ where τ is the dosing interval.

Downloaded from dmd.aspetjournals.org at ASPET Journals on June 18, 2019

TABLE 2. IC_{50} values (μM) for seven drugs vs six pooled recombinant CYP enzymes.

	CYP1A2	CYP2C8	CYP2C9	CYP2C19	CYP2D6	CYP3A4
Bupropion	> 50	> 50	> 50	4.84	7.11	> 50
Diltiazem	> 50	> 50	> 50	> 50	21.2	11.6
Fluoxetine	> 50	> 50	> 50	0.436	0.793	15.8
Itraconazole	> 50	14.9	> 50	6.0	> 50	0.319
Amiodarone	> 50	45	> 50	29.5	16.6	26.9
Citalopram	> 50	> 50	> 50	> 50	28.6	> 50
Gemfibrozil	> 50	27.2	22.7	8.66	> 50	> 50

DMD Fast Forward. Published on June 6, 2016 as DOI: 10.1124/dmd.116.071084
This article has not been copyedited and formatted. The final version may differ from this version.

Downloaded from dmd.aspetjournals.org at ASPET Journals on June 18, 2019

DMD Fast Forward. Published on June 6, 2016 as DOI: 10.1124/dmd.116.071084
This article has not been copyedited and formatted. The final version may differ from this version.

Figure 1

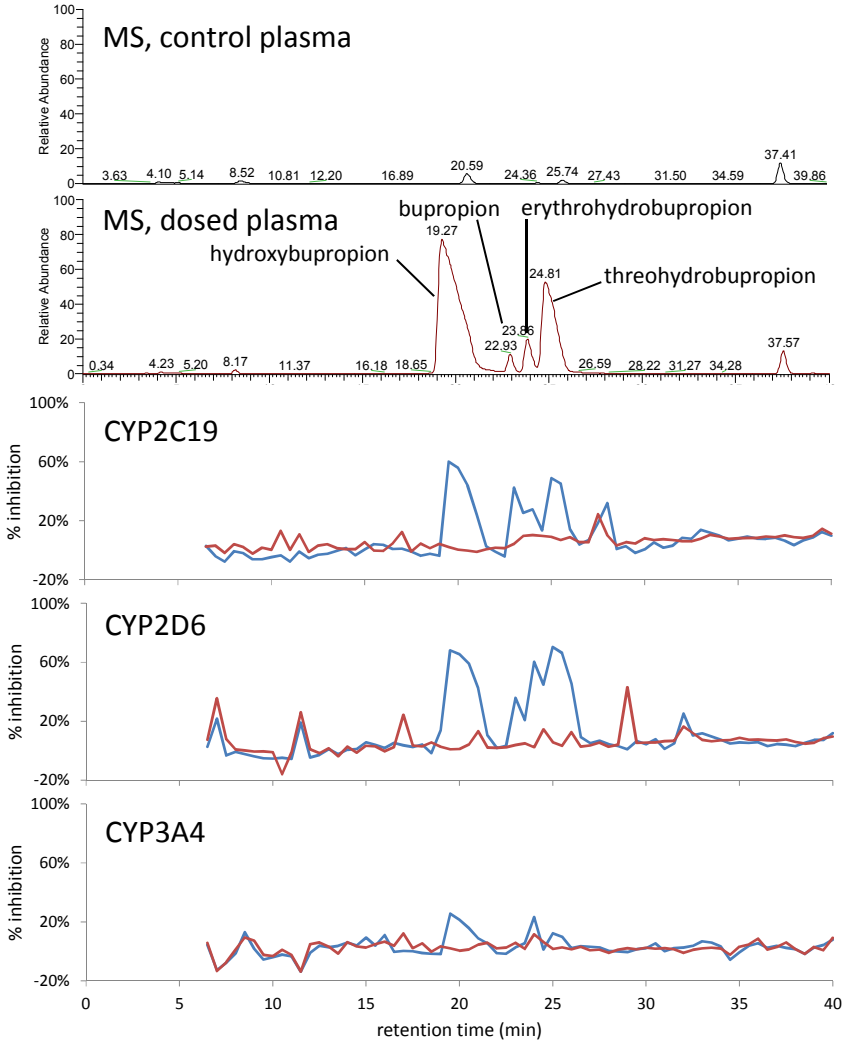

Downloaded from dmd.aspetjournals.org at ASPET Journals on June 18, 2019

DMD Fast Forward. Published on June 6, 2016 as DOI: 10.1124/dmd.116.071084
This article has not been copyedited and formatted. The final version may differ from this version.

Figure 2

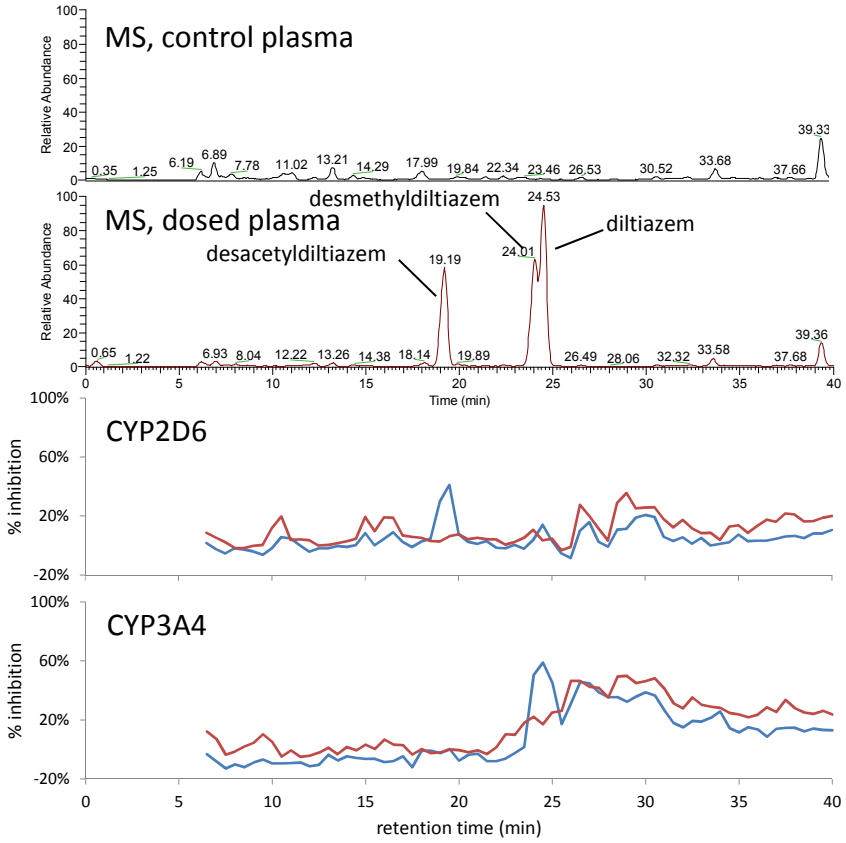

Downloaded from dmd.aspetjournals.org at ASPET Journals on June 18, 2019

DMD Fast Forward. Published on June 6, 2016 as DOI: 10.1124/dmd.116.071084
This article has not been copyedited and formatted. The final version may differ from this version.

Figure 3

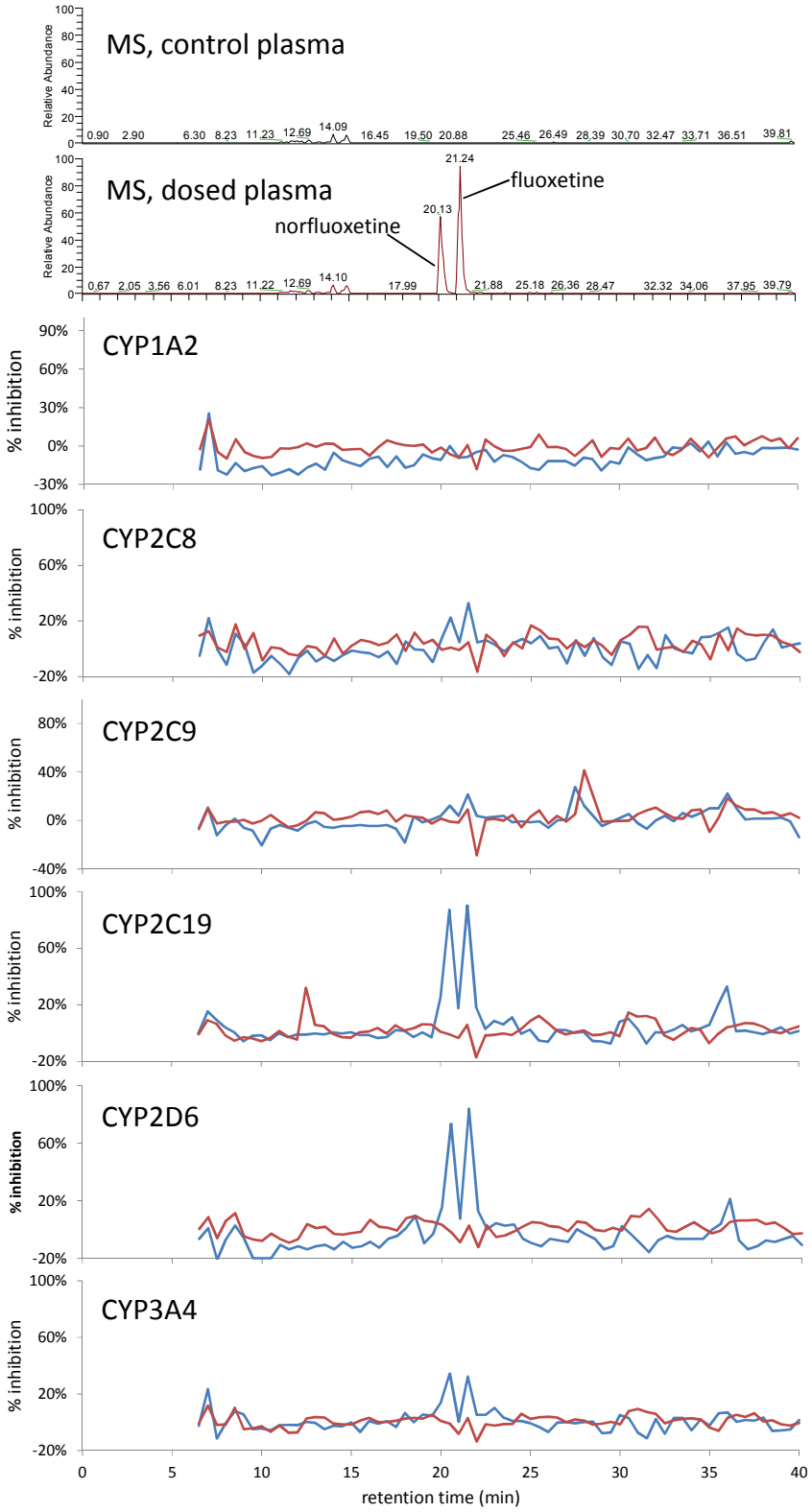

Downloaded from dmd.aspetjournals.org at ASPET Journals on June 18, 2019

DMD Fast Forward. Published on June 6, 2016 as DOI: 10.1124/dmd.116.071084
This article has not been copyedited and formatted. The final version may differ from this version.

Figure 4

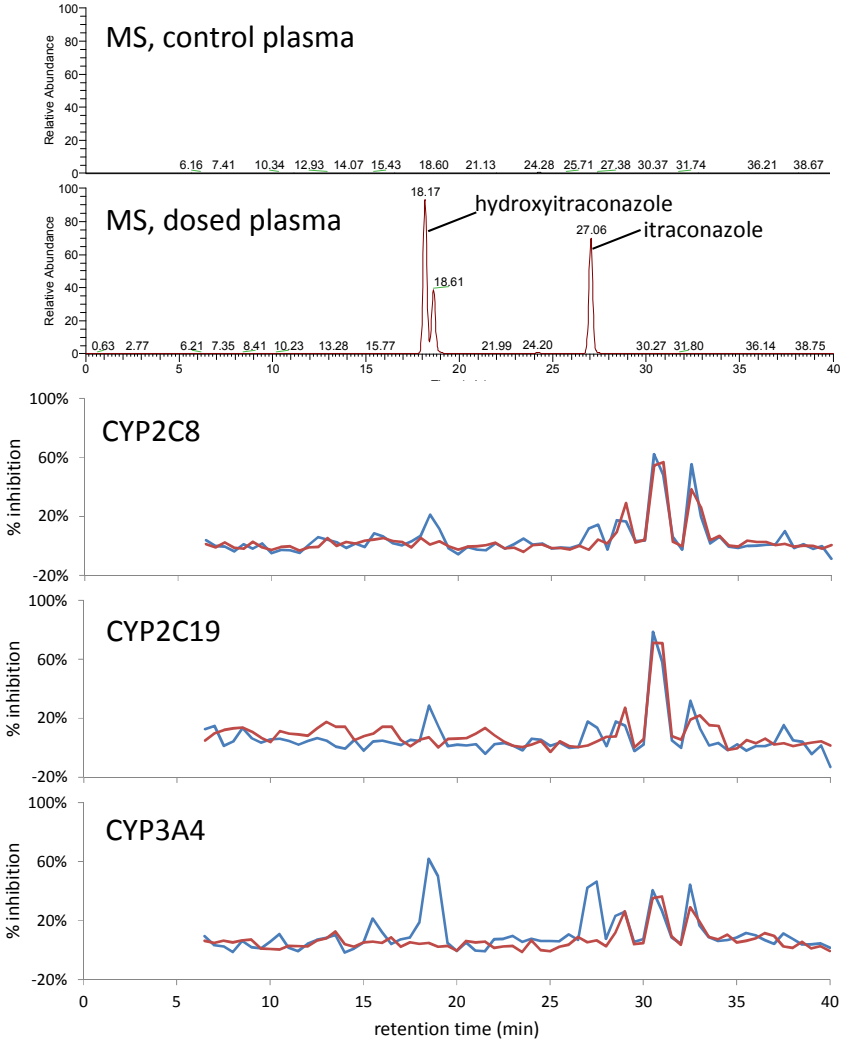

Downloaded from dmd.aspetjournals.org at ASPET Journals on June 18, 2019

DMD Fast Forward. Published on June 6, 2016 as DOI: 10.1124/dmd.116.071084
This article has not been copyedited and formatted. The final version may differ from this version.

Figure 5

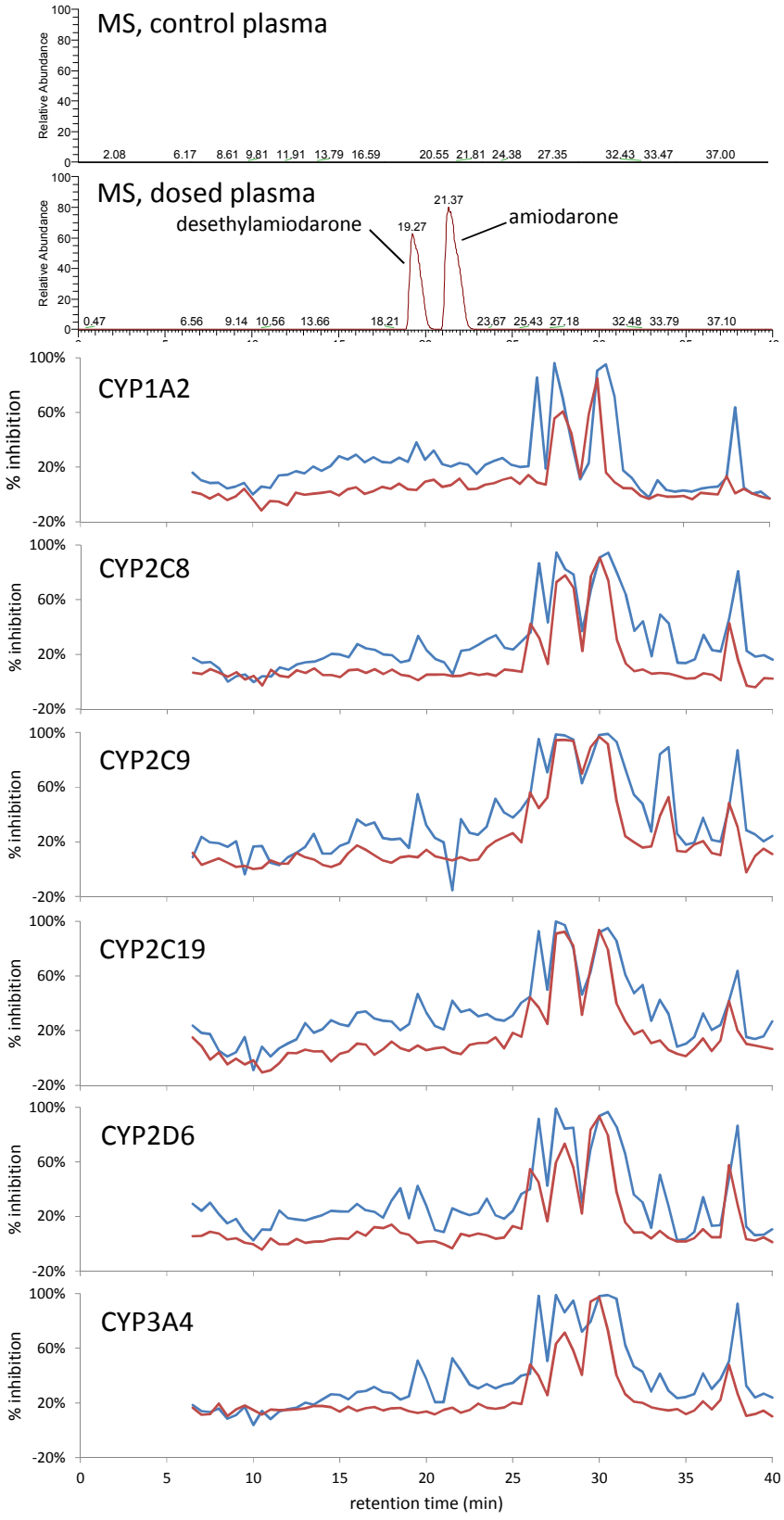

Downloaded from dmd.aspetjournals.org at ASPET Journals on June 18, 2019

DMD Fast Forward. Published on June 6, 2016 as DOI: 10.1124/dmd.116.071084
This article has not been copyedited and formatted. The final version may differ from this version.

Figure 6

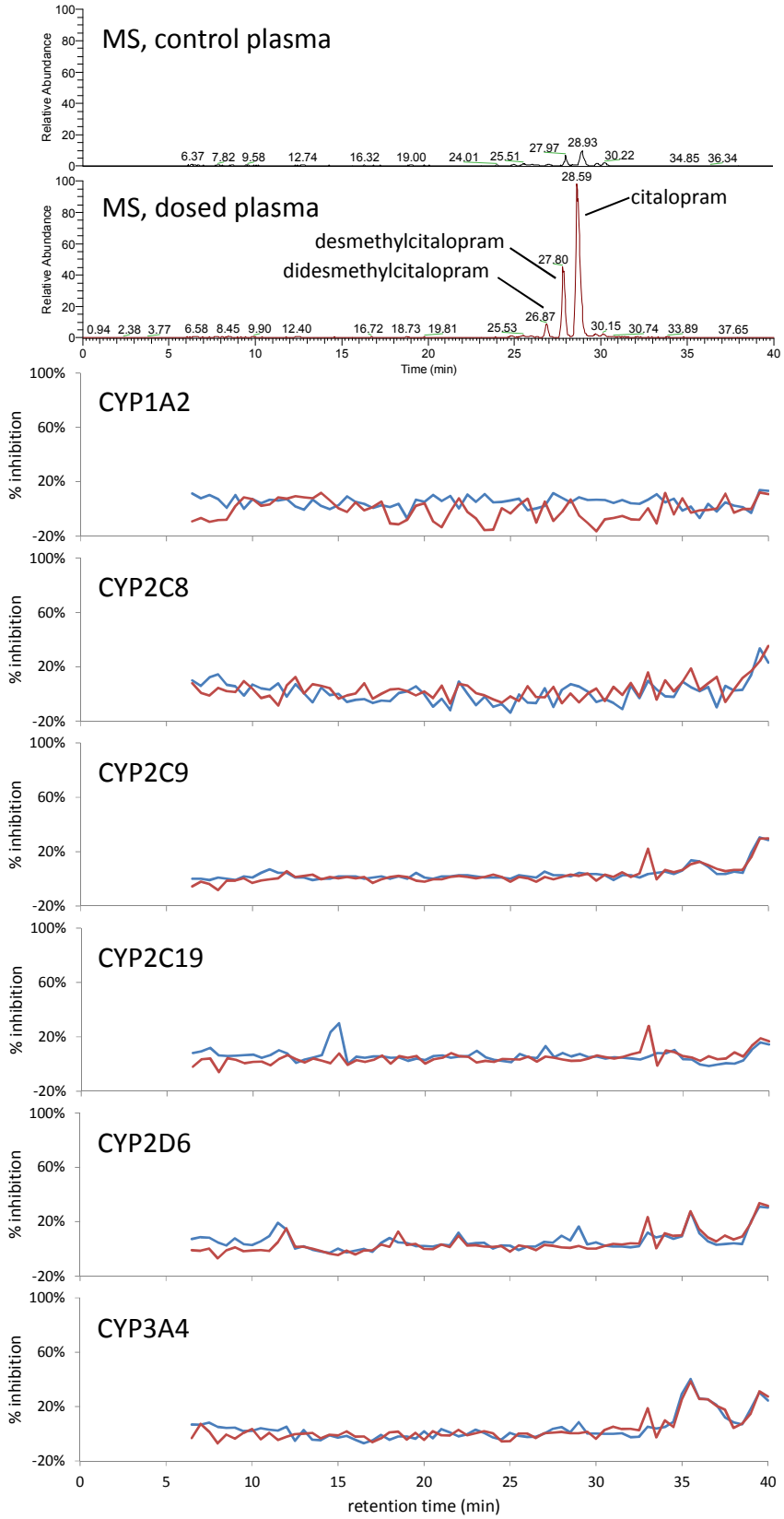

Downloaded from dmd.aspetjournals.org at ASPET Journals on June 18, 2019

DMD Fast Forward. Published on June 6, 2016 as DOI: 10.1124/dmd.116.071084
This article has not been copyedited and formatted. The final version may differ from this version.

Figure 7

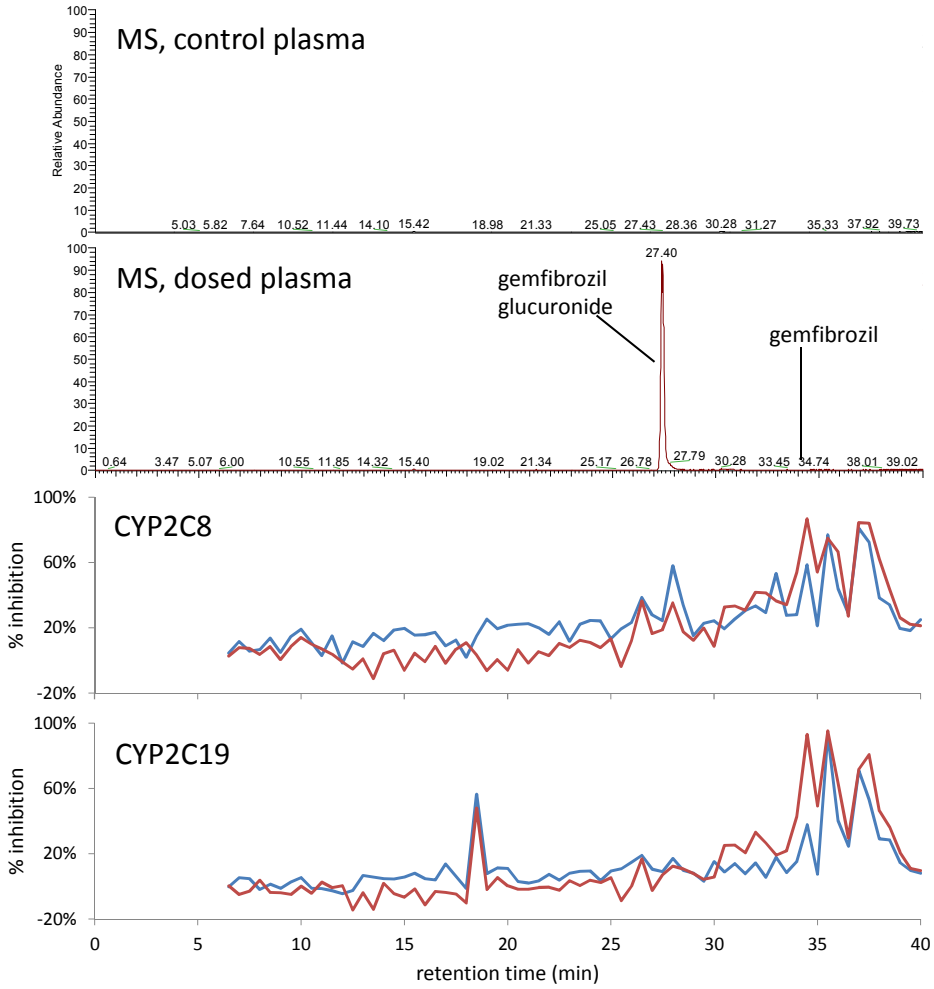

Downloaded from dmd.aspetjournals.org at ASPET Journals on June 18, 2019

Figure 8

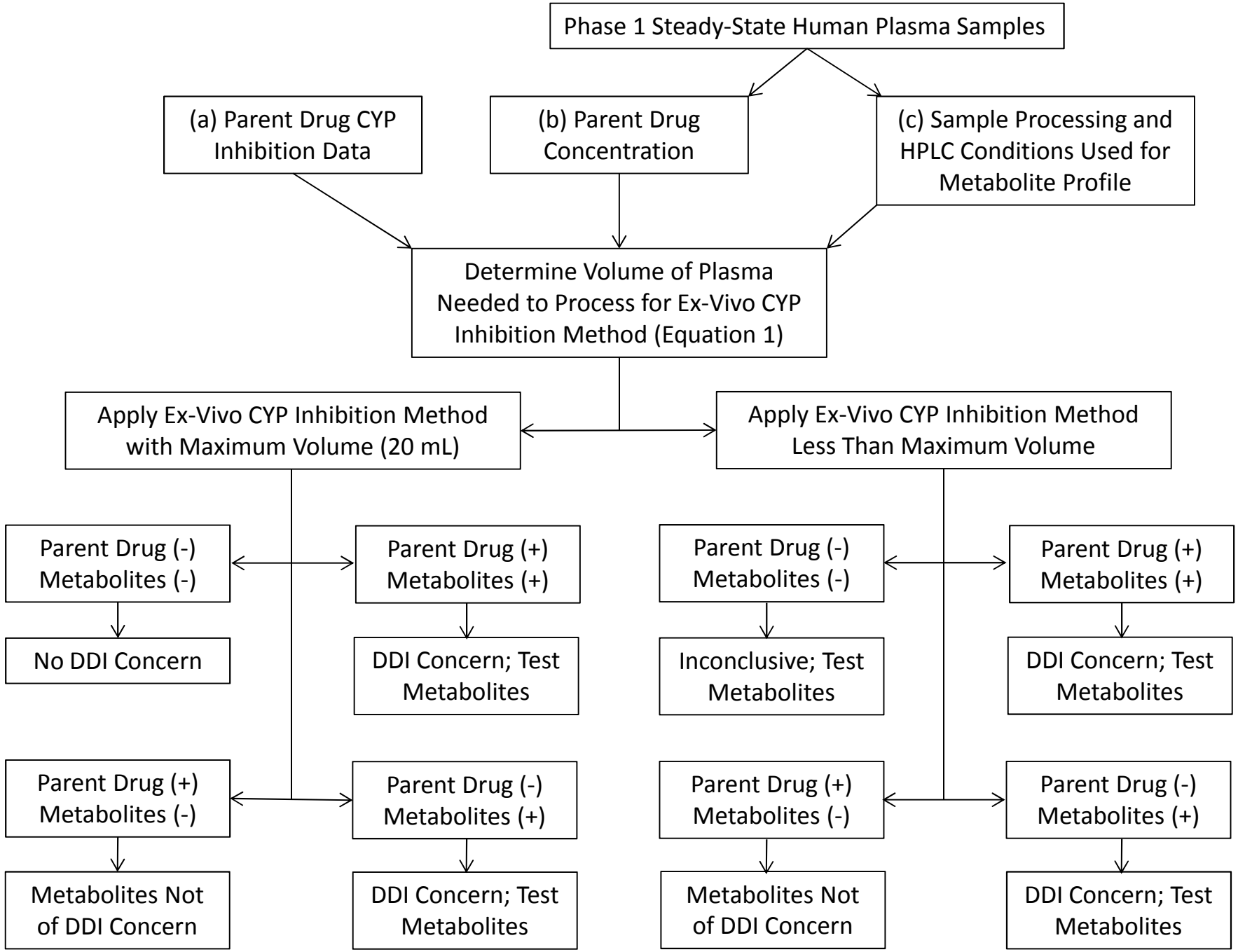

DMD Fast Forward. Published on June 6, 2016 as DOI: 10.1124/dmd.116.071084
This article has not been copyedited and formatted. The final version may differ from this version.

Downloaded from dmd.aspetjournals.org at ASPET Journals on June 18, 2019